Supporting Information for

Breaking the challenge of signal integrity using time-domain spoof surface plasmon polaritons

Hao Chi Zhang [†], Tie Jun Cui [†,%,*], Qian Zhang [†], Yifeng Fan [†], and Xiaojian Fu [†]

[†] *State Key Laboratory of Millimeter Waves, Southeast University, Nanjing 210096, China*

[%] *Cooperative Innovation Centre of Terahertz Science, No.4, Section 2, North Jianshe Road, Chengdu 610054, China*

This PDF file includes:

The detailed descriptions of 1) smooth conversions between the plasmonic waveguide and microstrip line; 2) eigen modes and excited modes of the plasmonic waveguide; 3) numerical results of two closely-packed single-strip SPP waveguides; and 4) the effects of dielectric substrate thickness and fault tolerance.

Figure S1. The geometry configuration of smooth conversions between the SPP waveguide and microstrip line.

Figure S2. The eigen-mode results of SPP waveguides with (**a**) different phase shifts, and (**b**) different groove depths *d*.

Figure S3. Simulated results of two closely-packed single-strip SPP waveguides, from which strong mutual coupling is observed. (**a**) The overall structure. (**b**) The simulated S-parameters. (**c**) The simulated time-domain signal spectra.

Figure S4. Simulated results of the spoof SPP waveguide. (**a**) Dispersion diagrams for different substrate thicknesses. (**b**) Dispersion diagrams for different relative shifts between the two corrugated structures along the wave propagation direction.

Smooth conversions between the plasmonic waveguide and microstrip line

Aimed to achieve the transition from the conventional microstrip line to plasmonic waveguide, two structures have been proposed[1-2], which can efficiently motivate the SPP modes by the microstrip line. In consideration of the feature of double-strip structure (the right subfigure in Fig. (S1)), we have improved the design in Ref. (2) and optimize all geometrical parameters to realize smooth conversions between the plasmonic waveguide and microstrip, in which the geometrical parameters are designed as: L_1=8 mm, L_2=40 mm, L_3=40 mm, w_1=1.588 mm and w_2=12 mm, as shown in Fig. (S1).

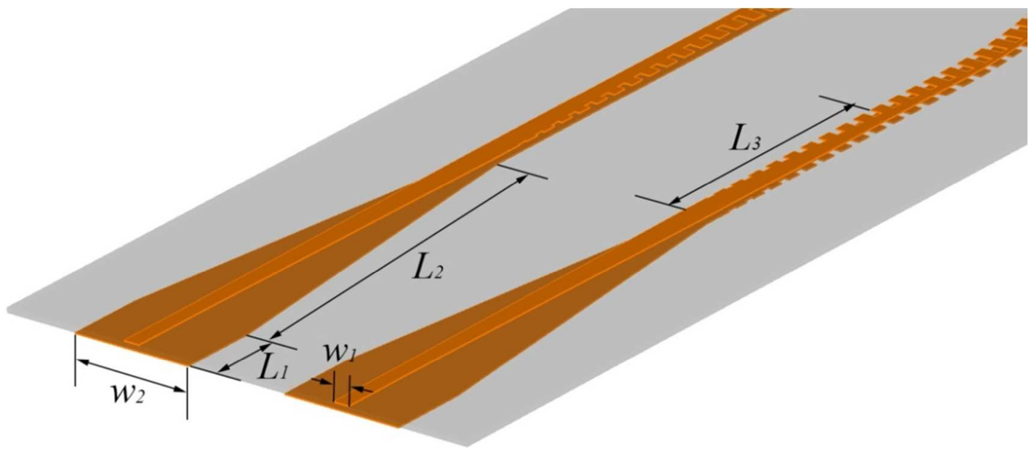

Figure S1. The geometry configuration of smooth conversions between the SPP waveguide and microstrip line.

Eigen modes and the excited modes of the plasmonic waveguide

In Ref. 2, we proposed a double-strip structure to support SPP modes. However, it does not satisfy the requirement of time-domain SPPs due to the lake of spectrum from 0.3 to 3.1 GHz[2]. Based on the mode-field distribution, the lake of spectrum is caused by the non-smooth conversions between the gap SPP mode and SPP mode. Hence we improve our design to overcome the problem by optimizing the scaling relation of geometrical parameters. For clearly showing the electric distribution of spoof SPPs, we provide the front-view figure of eigen modes (Fig. (S2a)). We notice that the field distribution is transposed from the gap SPP mode to surface-wave mode. This special phenomenon is caused by the gradually enhanced field confinement abilities of the metallic grooves. According to the dispersion curve of spoof SPPs, the confinement ability can also be tuned by changing the geometry parameters (e.g.

groove depths *d*). Hence we can realized the gap SPP mode and SPP mode at the required frequencies, as shown in Fig. (S2b), which can be utilized to excite the SPP mode. Compared to the SPP mode, the smooth conversions between the gap SPP mode and spatial mode in microstrip are more easily to achieve due to the similar field distributions in the plane perpendicular to the propagating direction.

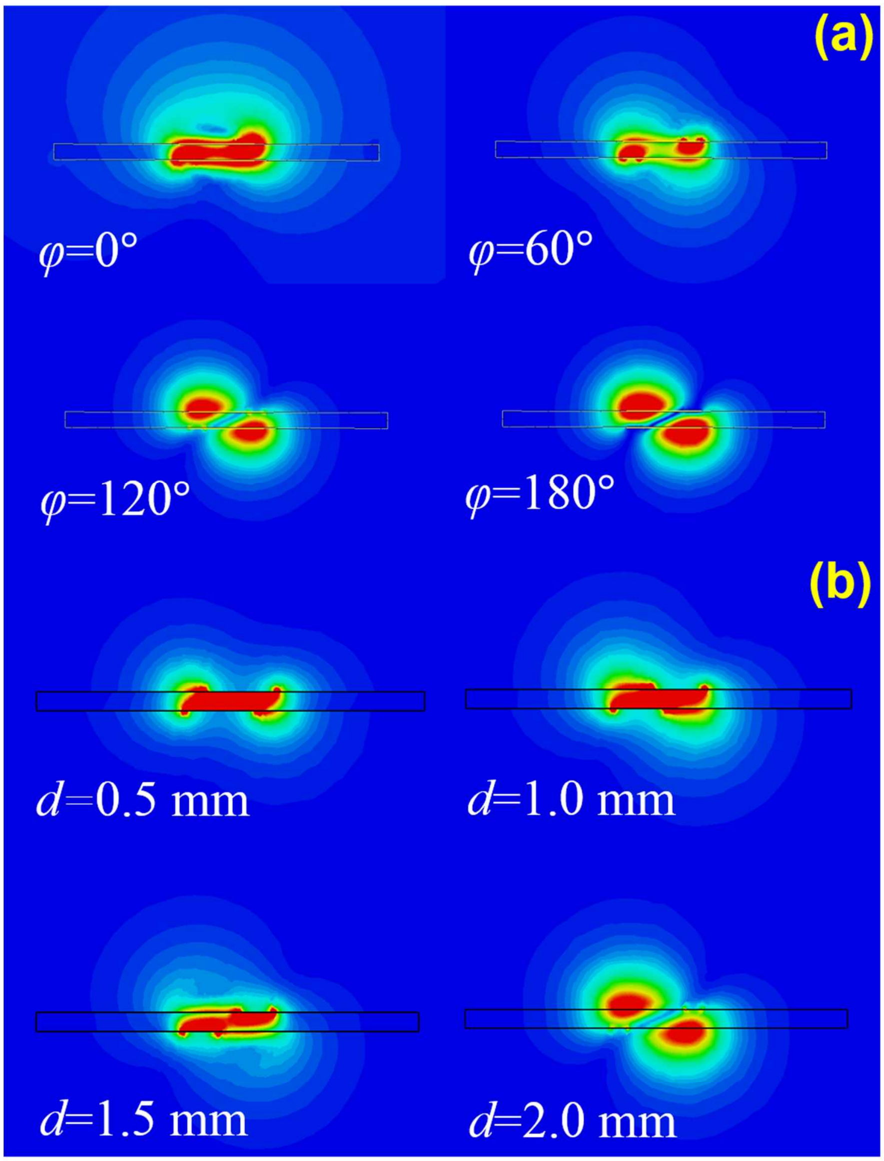

Figure S2. The eigen-mode results of SPP waveguides with (**a**) different phase shifts, and (**b**) different groove depths *d*.

Numerical results of two closely-packed single-strip SPP waveguides

As one of most potential candidates of conformal circuits, conformal surface plasmons (CSPs)[3] and related functional devices[4-9] on single-strip waveguides have been intensively studied in recent years. Hence we select single-strip SPP waveguides as the other comparison, as shown in Fig. (S3a). The numerical results of S-parameters and time-domain spectra for two closely-packed single-strip SPP waveguides are illustrated in Figs. (S3b) and (S3c), respectively. We clearly observe that the adjacent waveguides behave like a spoof SPP coupler[9] rather than two non-interfering transmission lines. That is to say, the coupling coefficient κ of the single-strip structure is much larger than that of double-strip structure, which cannot be used to suppress the interactions between the two SPP waveguides.

The effects of dielectric substrate thickness and fault tolerance

For future engineering applications, we need to discuss the effect of dielectric substrate, such as the change of substrate thickness. From full-wave numerical simulations using the CST Microwave Studio, the eigen-mode results with different substrate thicknesses are illustrated in Fig. (S4a). We observe that the cut frequency will gradually increase as the thickness increases, which is caused by the decrease of coupling between the two narrow corrugated metallic strips.

On the other hand, the mechanic error is ubiquity in real applications, such as the relative shift between the two corrugated strips along the wave propagation direction. For quantitative analyses, we give the numerical simulation results of the double-strip structure with relative shifts, as shown in Fig. (S4b). We obviously see that the dispersion curves do not exhibit significant changes in the transmission bands with different shifts, implying that the double-strip structure has a high fault tolerance.

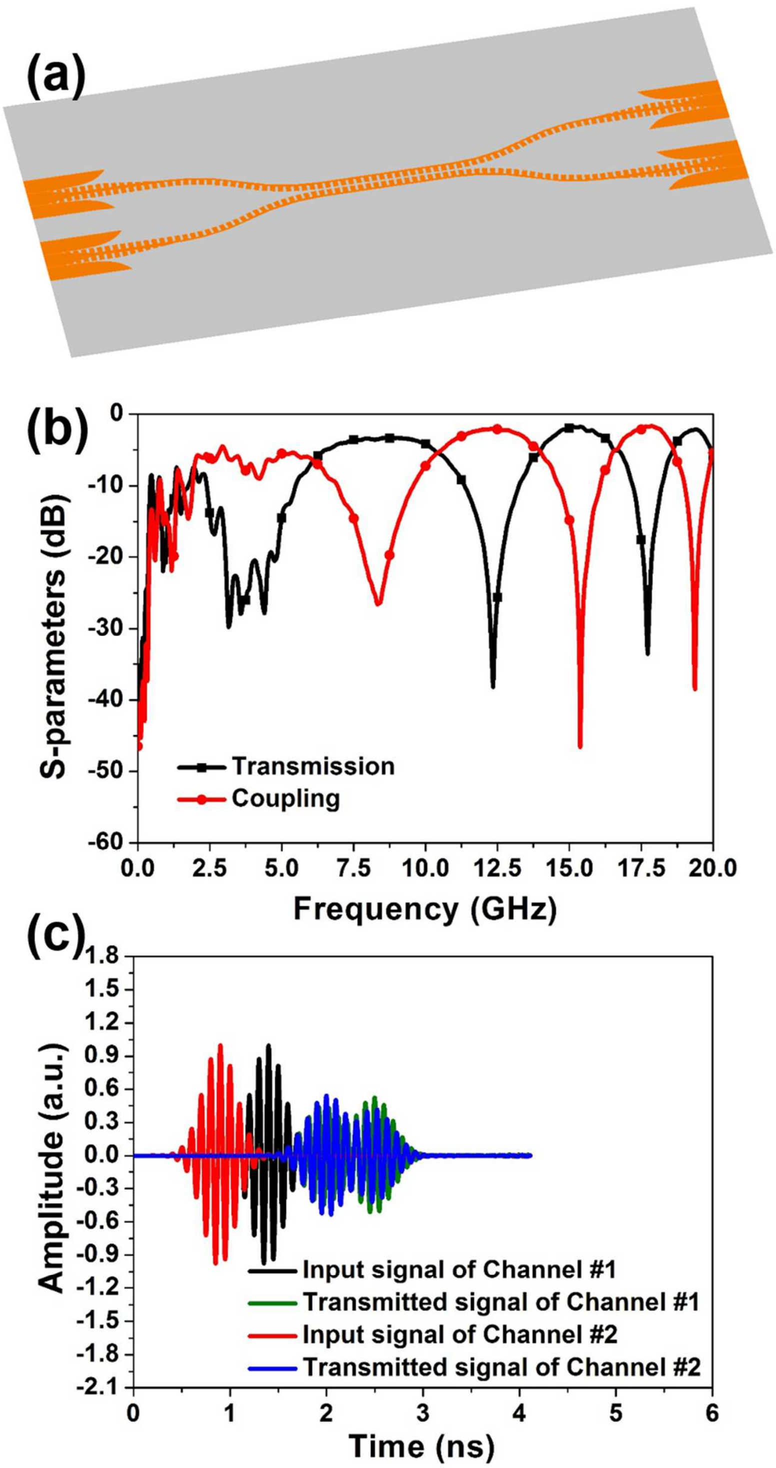

Figure S3. Simulated results of two closely-packed single-strip SPP waveguides, from which strong mutual coupling is observed. (**a**) The overall structure. (**b**) The simulated S-parameters. (**c**) The simulated time-domain signal spectra.

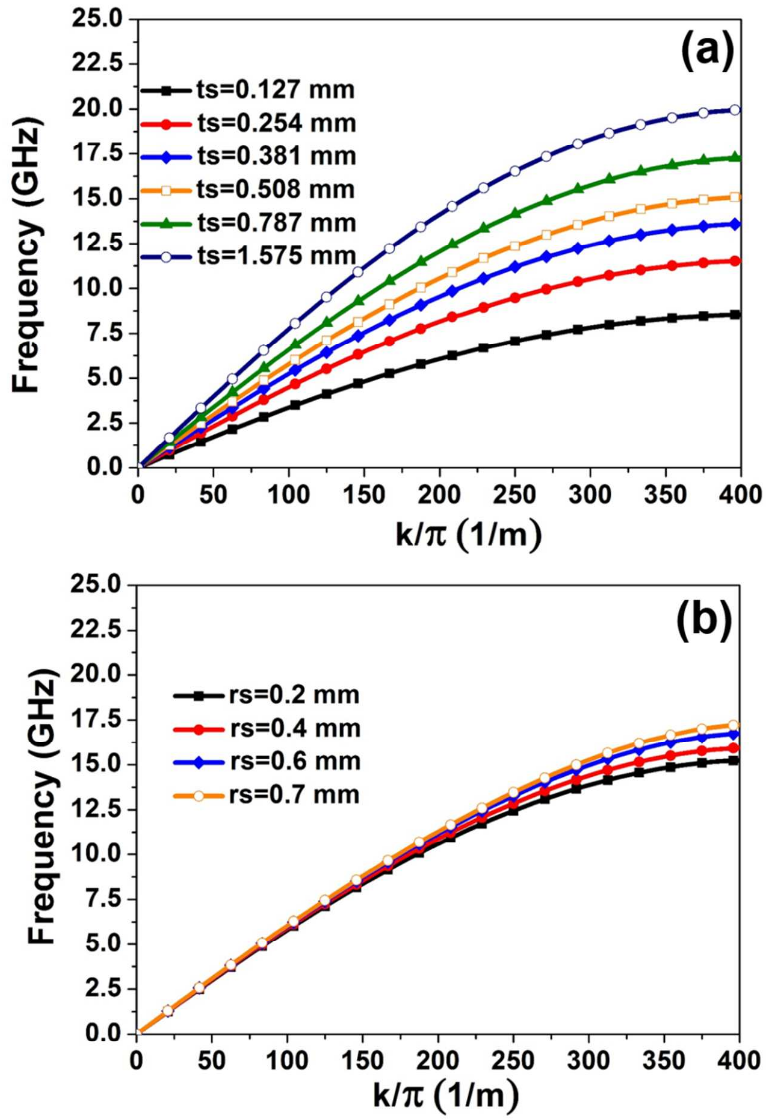

Figure S4. Simulated results of the spoof SPP waveguide. (**a**) Dispersion diagrams for different substrate thicknesses. (**b**) Dispersion diagrams for different relative shifts between the two corrugated structures along the wave propagation direction.

REFERENCES

(1) Z. Liao, J. Zhao, B. C. Pan, X. P. Shen, T. J. Cui, Broadband transition between microstrip line and conformal surface plasmon waveguide, *J. Phys. D: Appl. Phys.* **47**, 315103 (2014).

(2) H. C. Zhang, S. Liu, X. Shen, L. H. Chen, L. Li, T. J. Cui, Broadband amplification of spoof surface plasmon polaritons at microwave frequencies. *Laser & Photon. Rev.* **9**,

83-90 (2015).

(3) X. Shen, T. J. Cui, D. Martin-Cano, F. J. Garcia-Vidal, Conformal surface plasmons propagating on ultrathin and flexible films. *P. Natl. Acad. Sci. USA.* **110**, 40-45 (2013).

(4) X. Gao, L. Zhou, Z. Liao, H. F. Ma, T. J. Cui, An ultra-wideband surface plasmonic filter in microwave frequencies, *Appl. Phys. Lett.* **104**, 191603 (2014).

(5) J. Y. Yin, J. Ren, H. C. Zhang, B. C. Pan, T. J. Cui, Broadband frequency-selective spoof surface plasmon polaritons on ultrathin metallic structure, *Sci. Rep.* **5**, 8165 (2013).

(6) X. Shen, and T. J. Cui, Planar plasmonic metamaterial on a thin film with nearly zero thickness, *Appl. Phys. Lett.* **102**, 211909 (2013).

(7) J. J. Xu, H. C. Zhang, Q. Zhang, T. J. Cui, Efficient conversion of surface-plasmon-like modes to spatial radiated modes, *Appl. Phys. Lett.* **106**, 021102 (2015).

(8) B. C. Pan, Z. Liao, J. Zhao, T. J. Cui, Controlling rejections of spoof surface plasmon polaritons using metamaterial particles, *Opt. Express* **22**, 13940 (2014).

(9) X. Liu, Y. Feng, K. Chen, B. Zhu, J. Zhao, T. Jiang, Planar surface plasmonic waveguide devices based on symmetric corrugated thin film structures, *Opt. Express* **22**, 20107 (2014).